Proceedings of the 26th International Conference on
Port and Ocean Engineering under Arctic Conditions
June 14-18, 2021, Moscow, Russia

Numerical analysis of two different types of icebreaker bows breaking ice by the particle method

Yuan Zhang[1], Chao Wang[1], Liyu Ye[1], Longbin Tao[2]
[1] Harbin Engineering University, Harbin, China
[2] University of Strathclyde, Glasgow, United Kingdom

ABSTRACT

The present work studies the process of two different types of icebreaker bows, the unconventional bow and the conventional bow, breaking level ice. Based on the particle method and contact theory, the ice-bow interaction model is established. The ice is treated as an elastic material, and the icebreaker bow is regarded as an undeformed rigid body. Then, the icebreaking process of two icebreaker bow is simulated. The results show that The bow shape greatly determines the icebreaking pattern. The conventional icebreaker with extreme bow shape has multiple forms of crack growth, including radial crack and three circumferential cracks, while the moderate-shaped Thyssen WAAS bow has concise crack propagation pattern with neat circumferential crack and radial crack.

KEY WORDS: Particle method, Icebreaker bow, Icebreaking loads.

INTRODUCTION

The bow shape of the icebreakers has a significant influence on icebreaking ability. As stated by Sodhi (1995): the conventional bows (which are usually shaped in blunt wedge and has sharp stem), such as Straight stem with parallel buttock, Concave stem (white bow), and Melville bow, are advantageous in breaking ice rather than clearing broken ice floes in an open channel; on contrast, unconventional bows (which are different from conventional bows) with moderate profile, such as Spoon bow with reamers, Semi-spoon bow with chines, Flat family, and Thyssen-Waas bow, have better overall performance and especially excellent operating performance in pushing rubble ice and clearing broken ice pieces. For instance, European icebreaker Orden, the modification of Spoon bow with reamers, extends beam at the shoulder with the abrupt change in shape, eliminating the midship resistance. Regarding that different icebreaker bows show diverse characteristics when interacting with ice, a good-understanding study on the difference in the bow-ice interaction process between different bows will contribute to the bow selection for ice navigation.

In the numerical study on the ice-ship interaction, much work has been done to capture the further physical process of ice-ship interaction, which was reviewed in a very recent article (Xue et al., 2020). Of all the methods reviewed in Xue et al. (2020), the meshfree particle methods, such as Smoothed Particle Hydrodynamics (SPH) and Peridynamics (PD),

demonstrated their superior and robust potential to solve ice damage problems. The PD method especially predicts the evolution of crack propagation in ice failure realistically and accurately with its own fracture criterion. This was well demonstrated by previous work: ice-propeller interaction (Wang et al., 2018; Ye et al., 2017), submarine surfacing through ice (Ye et al., 2020), and ice-structure interaction (Vazic et al., 2019). Therefore, the meshfree particle method, PD, is utilised as the basic methodology for the ice model in the present paper.

The model was first constructed by Zhang et al. (2021a). The comprehensive verification of the numerical model has also been carried out by comparing the icebreaking resistance with different ship velocities (Zhang et al., 2021a). The present paper investigates the differences in the icebreaking process between the conventional bow and unconventional bow by particle method, Peridynamics. The ice failure, icebreaking pattern, ice loads, and icebreaking cycle are analysed. The results show that the outline of the icebreaker bow has great influences on the icebreaking process.

Peridynamics

Peridynamics (PD) is a nonlocal method, which provides a more practical particle method to simulate large-scale failure and deformation from a macro perspective. The PD discretises the continuous medium into uniform/nonuniform material points, as shown in Figure 1. In the reference coordinate system, the motion equation of the material point in PD theory is (Madenci and Oterkus, 2014):

$$\rho(\mathbf{x})\ddot{\mathbf{u}}(\mathbf{x},t)=\int_{H_X}\left\{\underline{\mathbf{T}}\left[\mathbf{x},t\right]\left\langle\mathbf{x}'-\mathbf{x}\right\rangle-\underline{\mathbf{T}}\left[\mathbf{x}',t\right]\left\langle\mathbf{x}-\mathbf{x}'\right\rangle\right\}dV_{x'}+\mathbf{b}(\mathbf{x},t) \tag{1}$$

wherein H_x is the horizon constructed by the material points in the family of material particle $\mathbf{x}$. The size of the horizon is δ. $\mathbf{u}$ and $\mathbf{u}'$ are the displacement of particle $\mathbf{x}$ and its' neighbour $\mathbf{x}'$. When the body deformed, their new position are $\mathbf{y}$ and $\mathbf{y}'$. $\rho(\mathbf{x})$ is ice density. $\mathbf{T}$ is the force density between two particles. The direction of force density between two particles is opposite, and the direction points to each other. The force between two particles is two different force densities, they are $\underline{\mathbf{T}}\left[\mathbf{x},t\right]$ and $\underline{\mathbf{T}}\left[\mathbf{x}',t\right]$, respectively.

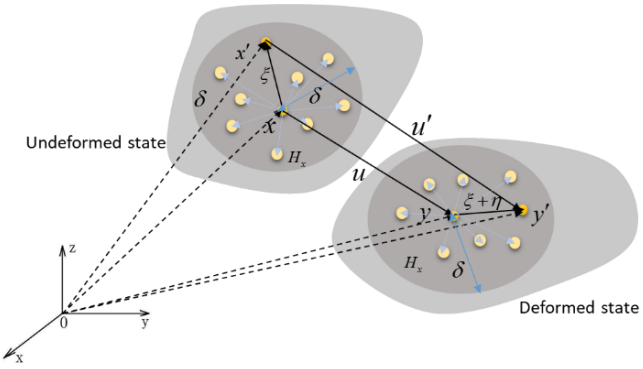

Figure 1. Interaction of a material point $\mathbf{x}$ with its neighbouring points

Comparing the relationship between strain energy density and force density with the corresponding relationship in classical medium mechanics, the force density in the PD method can be deduced. Then the detailed integral expression of PD can be obtained (Gao and Oterkus, 2018):

$$\rho(\mathbf{x})\ddot{\mathbf{u}}(\mathbf{x},t)=\int_{H_X}\left\{\frac{2\delta d\Lambda a}{|\mathbf{x}'-\mathbf{x}|}(\theta+\theta')+4\delta bs\right\}\frac{\mathbf{y}'-\mathbf{y}}{|\mathbf{y}'-\mathbf{y}|}dV_{x'}+\mathbf{b}(\mathbf{x},t) \tag{2}$$

in which a, d and b are PD parameters. Λ is the aulixary parameters. θ and θ' are dilatations of two interaction material points. s is the stretch. $\mathbf{b}$ is the external force。 s is an important variable and is extended to set up failure criterion. When s exceeds the ultimate elongation of the material, the material will be destroyed, and the failure process is irreversible. μ is a historical scalar presenting the material damage, that is (Ye et al., 2019):

$$\mu(t,\xi)=\begin{cases}1\ if\ \ s(t',\xi)<s_0\ \ for\ all\ \ 0\le t'\le t\\ 0\ otherwise\end{cases} \tag{3}$$

In order to quantify the ice failure and present the crack propagation, a quantity known as local damage is proposed as:

$$\varphi(\mathbf{x},t)=1-\frac{\int_{H_x}\mu(t,\xi)dV_\xi}{dV_\xi} \tag{4}$$

The value of $\varphi(\mathbf{x},t)$ is between 0-1, and the closer to 1, the greater the degree of the ice damage. $\mu(t,\xi)$ is the history-dependent scalar-valued function.

CONTACT MODEL

In the present work, the ice-ship interaction model is a contact process between a rigid hull body, whose deformation at any instant is not considered, and an ice object which is discretised into particles and governed by the PD equation. Therefore, the ice-ship contact needs to be detected first to calculate interpenetration.

Unlike regular objects such as spheres and cylinders, a ship's profile (especially the bow) is complex. This leads to it more difficult to detect the contact between two bodies or find specific impact particles. In order to solve the described issue and provide an efficient way to detect contact between particles and the impactor in an arbitrary shape. A contact detect model based on geometric graphics is presented here, which can be extended to model impact problems for any meshfree particle method.

The idea of the contact model is mainly composed of two parts, as shown in Figure 2. The first part is to create a bounding box containing the whole ship to reduce the unnecessary cost of particles search; the second part is developing an algorithm to search the particles inside the bounding box to find exact contacting particles relocate them. The implementation of each part is also shown in Figure 2.

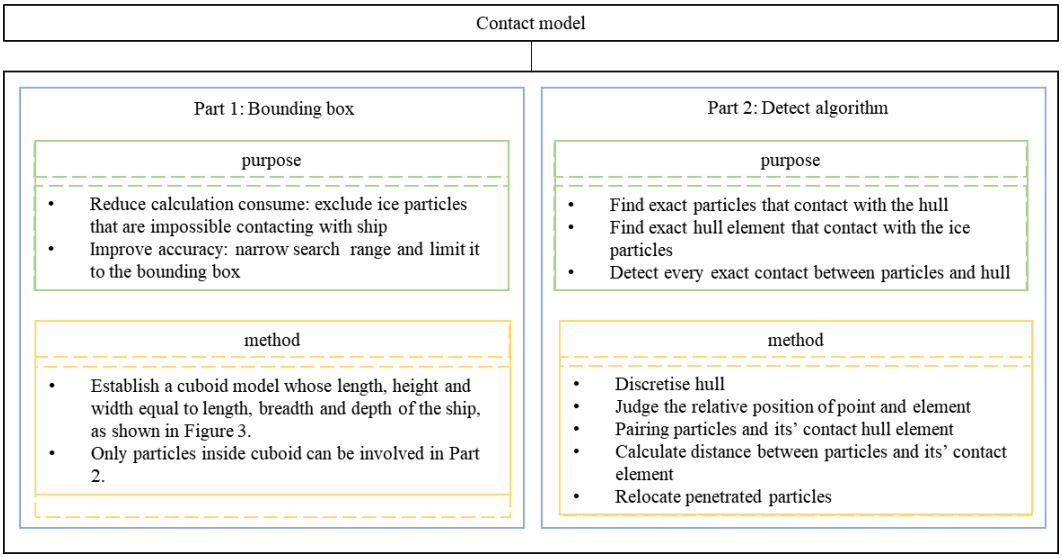

Figure 2. The framework of the contact model

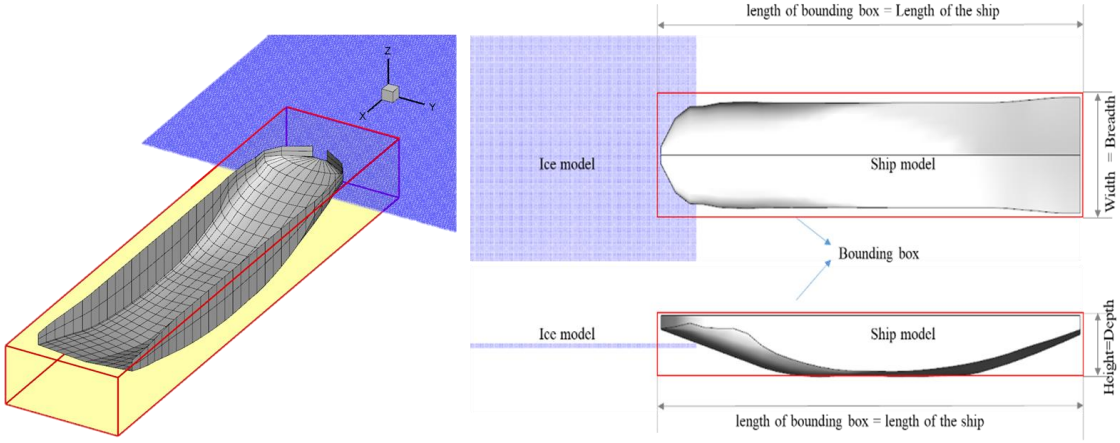

Figure 3. the bounding box

The information given about the contact model in this section is just a brief overview, and more technical information can be found in Zhang et al. (2021b). After the determination of particle contact, the particle redistribution position can be obtained:

$$\mathbf{x}^{t+\Delta t} = \mathbf{x}^{t} + V_0 \cdot \Delta t + d \cdot \mathbf{n} \tag{5}$$

Wherein d is the distance between particle and plane. $\boldsymbol{n}$ is the normal vector of the element plane of the hull, which is determined according to Vazic (2020). The velocity of the redistributed particle in its new location is calculated as:

$$\mathbf{v}^{t+\Delta t} = \frac{\mathbf{u}^{t+\Delta t} - \mathbf{u}^{t}}{\Delta t} \tag{6}$$

The force exerted on the target by the contact particle i is:

$$\mathbf{F}_{(i)}^{t+\Delta t} = -1 \times \rho_{(i)} \frac{\mathbf{v}_i^{t+\Delta t} - \mathbf{v}_i^{t}}{\Delta t} V_{(i)} \tag{7}$$

Summation of the contributions of all contacted material points results in the total reaction force, that is:

$$\mathbf{F}_{total}^{t+\Delta t} = \sum_{i=1} \mathbf{F}_{(i)}^{t+\Delta t} \lambda_{(i)}^{t+\Delta t} \tag{8}$$

Where $\lambda_{(i)}^{t+\Delta t}$ indicates the contact state between particles and structure, and is :

$$\lambda_{(i)}^{t+\Delta t} = \begin{cases} 1 \text{ inside structure} \\ 0 \text{ outside structure} \end{cases} \tag{9}$$

TWO DIFFERENT BOWS BREAK ICE

bow model and ice properties

The two typical icebreaker bows are a conventional bow from the Chinese icebreaker and an unconventional Thyssen-Waas bow from literature (Puntigliano, 1995). Their models are shown in Figure 4, and their principle dimensions are shown in Table 1. The model scale ratio is set to 1:25 in the numerical simulation.

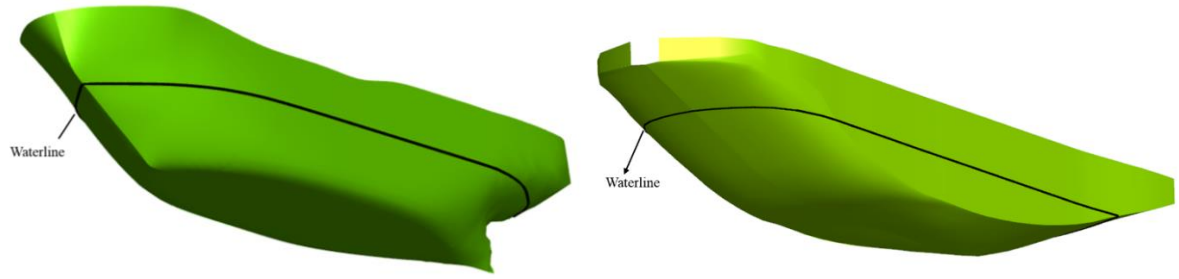

Figure 4. Numerical model of conventional icebreaker bow (left) and unconventional icebreaker bow (right)

Table 1. Principle dimension of two kinds of icebreaker

Items	Symbol/unite	Conventional bow		Unconventional bow	
		Full scale	Model scale	Full scale	Model scale
Length between perpendiculars	L_{pp}/m	147.2	5.888	100.0	4.0
Breadth	B/m	23.0	0.92	20.0	0.8
Depth	D/m	13.5	0.54	12.0	0.48
Draft	T/m	8.0	0.32	7.0	0.28
Flare angle	Ψ/deg	33	33	77	77
Waterline angle	β/deg	22	22	39	39
Buttock angle	φ/deg	28	28	13	12
Stem angle	α/deg	24.35	24.35	14	14
Bow length	L_f/m	32.5	1.3	10.0	0.4

The ice properties are: density $\rho = 826.6kg/m^3$, elastic modulus $E = 52.0 \times 10^6 Pa$, Poisson's ratio $v = 0.33$, critical stretch $s_0 = 0.0052$.

Icebreaking pattern and ice loads

Both icebreaker bows break level ice at a constant speed of 3 knots. A comparison of the icebreaking process of the conventional bow between experimental results and numerical simulation is shown in Figure 5.

As a verification analysis, the formation and propagation of the circumferential crack lead to bending failure when conventional bow breaking level ice. Bending is the dominant failure mode through the whole icebreaking process accompanied by a small amount of ice crushing. The icebreaking cycle follows a regular pattern: firstly, circumferential cracks are generated along the direction of the ship's length and continue to expand to both sides of the bow, and this type of cracks always start to form from the half-width position of the bow; As the ship advances, the circumferential cracks extend to the stern direction and stem direction. Radial cracks are generated accordingly; Then, the secondary cracks travel approximately parallel to the bow waterline. It is found that the numerical simulation well captured the icebreaking phenomenon observed in the experiment, as shown in Figure 5. Besides, as shown in Figure 7(a): the numerical calculation results are in good agreement with the experimental results and empirical formula results. Therefore, the numerical method established in this paper effectively simulates the icebreaking process.

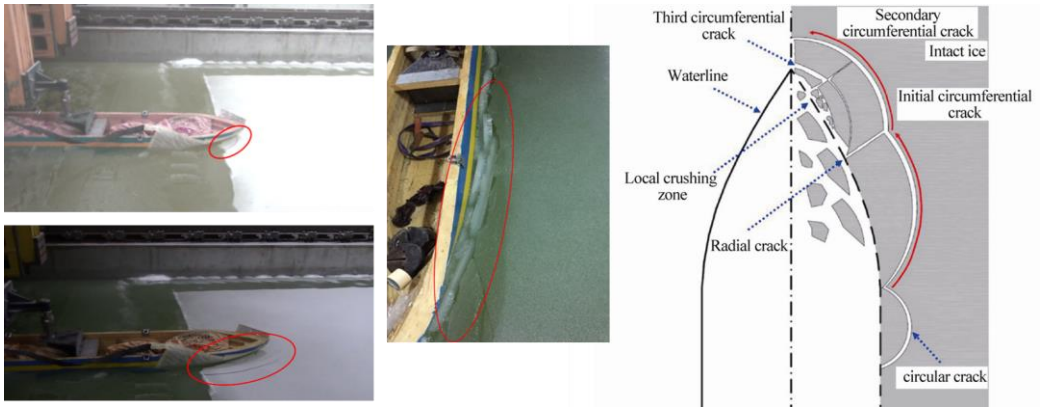

(a) experimental icebreaking process of conventional bow (Huang et al., 2018; Huang et al., 2016)

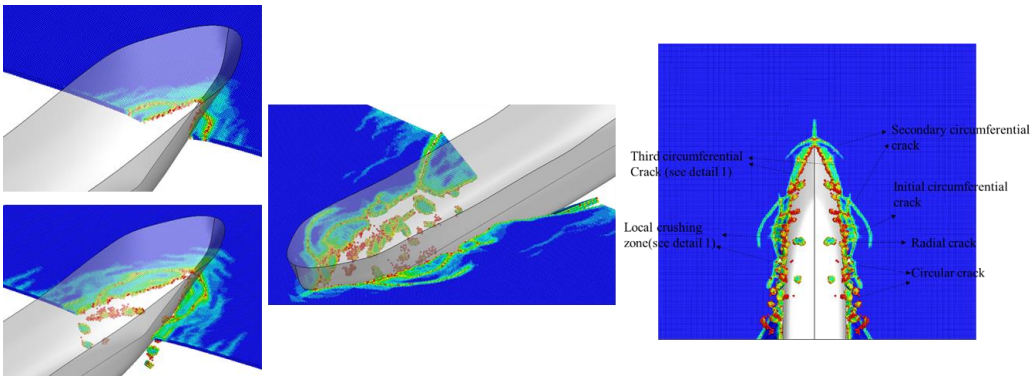

(b) Numerical simulation

Figure 5. Comparison between experimental results and numerical simulation

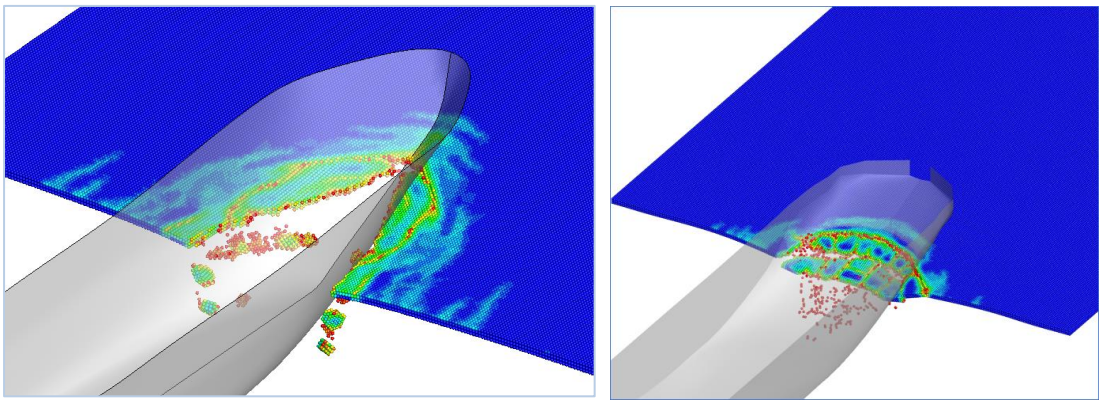

(a) Conventional bow (b) unconventional bow

Figure 6. The icebreaking process of two types of bows

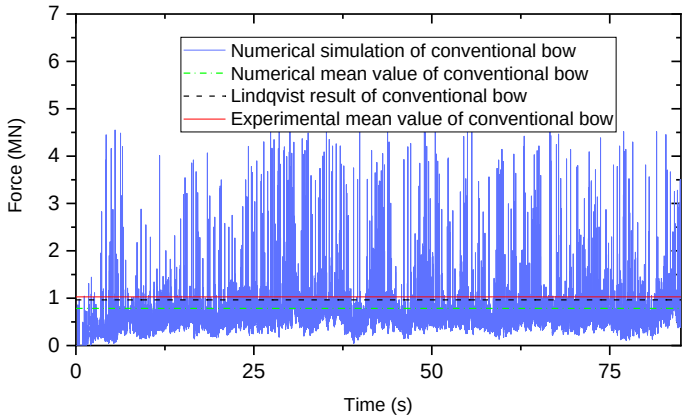

(a) Conventional bow

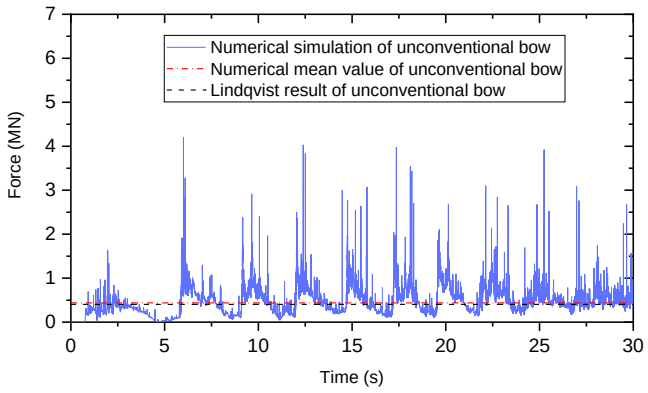

(b) unconventional bow

Figure 7. the icebreaking loads of two types of bows

The numerical results of the icebreaking process and icebreaking loads are depicted in Figure 6 and Figure 7. Comparing the icebreaking process of the conventional bow with that of the unconventional bow, it is noted that two kinds of icebreakers with different bows show significant differences both on ice failure mode and icebreaking loads. The comparison of the similarity and difference is analysed in Table 2.

Table 2. Comparison of icebreaking process between the traditional bow and the non-traditional bow

Items		Conventional bow	Unconventional bow
Ice failure	similarity	• Dominated by bending failure and accompanied by local crushing failure; • Mixed circumferential cracks and radial cracks.	
	difference	• The complex icebreaking process with varied circumferential cracks, such as first circumferential cracks and second circumferential cracks; • Fewer radial cracks; • Partial crack propagation occurs simultaneously with the previous crack	• Only one type of circumferential cracks; • More radial cracks; • The crack propagation takes place step by step.
Icebreaking cycle	similarity	A clear icebreaking cycle can be observed in the time history	
	difference	The icebreaking cycle partially coincide with the previous one	icebreaking cycles occur in sequence
Opening channel	-------	In the view of real scale, the breadth B of traditional bow icebreaker is 23.0 m, it's breaking channel is 28.56 m. The width of unconventional ship is 20.0 m, and it's breaking channel is 27.3 m. The relationship between channel width and ship breadth of the two ship types is 1.25B and 1.36B, respectively.	
Icebreaking loads	similarity	• There is a big difference between the maximum ice force and the minimum ice force; • The load trend corresponds to the icebreaking mode.	
	difference	Ice load is continuous.	The ice load has prominent periodic characteristics, and the ice load of each cycle first increases and then decreases.

CONCLUSIONS

In the present study, the Peridynamics and contact detection algorithm were employed to investigate the differences in the icebreaking process between two kinds of icebreaker bow, the conventional bow and the unconventional bow. The following conclusions are drawn:

(1) The bow shape has significant influences on the icebreaking process, including icebreaking pattern, crack propagation and width of the channel;
(2) Most of the cracks in the process of conventional bow breaking ice are circumferential cracks in different grades, while the radial cracks made up a huge part in the process of non-traditional bow breaking ice;
(3) The icebreaking load of the unconventional bow has apparent periodicity, which coincides with the icebreaking mode, while the icebreaking cycle of the conventional bow is not obviously distinct;
(4) The traditional icebreaker opens the channel by a sharp-shaped bow splitting the ice layer, while the bow of the traditional icebreaker breaks the ice layer mainly by gravity.

In this paper, only the icebreaking differences of the two categories of the bow were analysed. However, the study of the influence of bow shape parameters on icebreaking ability is the author's intention in the near future.

ACKNOWLEDGEMENTS

This work is sponsored by the National Natural Science Foundation of China (Nos. 51909043 and 51809055), the Natural Science Foundation of Heilongjiang Province of China (Grant NO. E2018026), and China Postdoctoral Science Foundation (Grant NO. 2020M681082 and 2019M651266).

REFERENCES

Nam, J.H., Sohn, S., & Singer, D.J., 2012. Estimation of geometry-based manufacturing cost of complex offshore structures in early design stage. *International Journal of Naval* Architecture and Ocean Engineering, 4(3), pp.291-301.

Gao, Y. & Oterkus, S. 2018. Ordinary state-based peridynamic modelling for fully coupled thermoelastic problems. Continuum Mechanics and Thermodynamics, 31(4), pp 907-937.

Huang, Y., Huang, S. Y. & Sun, J. Q. 2018. Experiments on navigating resistance of an icebreaker in snow covered level ice. Cold Regions Science and Technology, 152(1-14.

Huang, Y., Sun, J. Q., Ji, S. P. & Tian, Y. K. 2016. Experimental Study on the Resistance of a Transport Ship Navigating in Level Ice. Journal of Marine Science and Application, 15(2), pp 105-111.

Madenci, E. & Oterkus, E. 2014. Peridynamic Theory and Its Applications.

Sodhi, D. S. 1995. Northern Sea Route Reconnaissance Study: A Summary of Icebreaking Technology: DIANE Publishing.

Vazic, B., 2020. Multi-scale modelling of ice-structure interactions. University of Strathclyde.

Vazic, B., Oterkus, E., Oterkus, S., 2019. Peridynamic approach for modelling ice-structure interactions, Trends in the Analysis and Design of Marine Structures: Proceedings of the 7th International Conference on Marine Structures CRC Press, Dubrovnik, Croatia.

Wang, C., Xiong, W.P., Chang, X., Ye, L.Y., Li, X., 2018. Analysis of variable working conditions for propeller-ice interaction. Ocean Engineering 156, 277-293.

Xue, Y.Z., Liu, R.W., Li, Z., Han, D.F., 2020. A review for numerical simulation methods of ship-ice interaction. Ocean Engineering 215.

Ye, L. Y., Guo, C. Y., Wang, C., Wang, C. H. & Chang, X. 2019. Peridynamic solution for submarine surfacing through ice. Ships and Offshore Structures, 15(5), pp 535-549.

Ye, L.Y., Wang, C., Chang, X., Zhang, H.Y., 2017. Propeller-ice contact modeling with peridynamics. Ocean Engineering 139, 54-64.

Zhang, Y., Tao, L., Wang, C., Ye, L.Y., Guo, C.Y., 2021a. Numerical study on dynamic icebreaking process of an icebreaker by ordinary state-based Peridynamics and continuous contact detection algorithm. Ocean Engineering (in press).

Zhang, Y., Tao, L., Wang, C., Ye, L.Y., Sun, S., 2021b. Numerical study of icebreaking process with two different bow shapes based on developed particle method in parallel scheme. Applied Ocean Research (in press).